JOURNAL OF VIROLOGY, Jan. 2008, p. 461–470 Vol. 82, No. 1
0022-538X/08/$08.00+0 doi:10.1128/JVI.01894-07

Effect of Cell Polarization on Hepatitis C Virus Entry▽

Christopher J. Mee, Joe Grove, Helen J. Harris, Ke Hu, Peter Balfe,* and Jane A. McKeating

Division of Immunity and Infection, Institute for Biomedical Research, University of Birmingham, Birmingham, United Kingdom

Received 30 August 2007/Accepted 12 October 2007

The primary reservoir for hepatitis C virus (HCV) replication in vivo is believed to be hepatocytes within the liver. Three host cell molecules have been reported to be important entry factors for receptors for HCV: the tetraspanin CD81, scavenger receptor BI (SR-BI), and the tight-junction (TJ) protein claudin 1 (CLDN1). The recent discovery of a TJ protein as a critical coreceptor highlighted the importance of studying the effect(s) of TJ formation and cell polarization on HCV entry. The colorectal adenocarcinoma Caco-2 cell line forms polarized monolayers containing functional TJs and was found to express the CD81, SR-BI, and CLDN1 proteins. Viral receptor expression levels increased upon polarization, and CLDN1 relocalized from the apical pole of the lateral cell membrane to the lateral cell-cell junction and basolateral domains. In contrast, expression and localization of the TJ proteins ZO-1 and occludin 1 were unchanged upon polarization. HCV infected polarized and nonpolarized Caco-2 cells to comparable levels, and entry was neutralized by anti-E2 monoclonal antibodies, demonstrating glycoprotein-dependent entry. HCV pseudoparticle infection and recombinant HCV E1E2 glycoprotein interaction with polarized Caco-2 cells occurred predominantly at the apical surface. Disruption of TJs significantly increased HCV entry. These data support a model where TJs provide a physical barrier for viral access to receptors expressed on lateral and basolateral cellular domains.

Hepatitis C virus (HCV) is an enveloped positive-stranded RNA virus and the sole member of the *Hepacivirus* genus, within the family *Flaviviridae*. Worldwide, approximately 170 million individuals are infected with HCV and a significant fraction of these people are at risk of developing serious progressive liver disease. The principal reservoir for viral replication is believed to be hepatocytes within the liver. The recent development of the retrovirus pseudoparticle system (HCVpp) (5, 25) and the ability of the JFH-1 strain of HCV to release infectious particles in cell culture (HCVcc) (30, 45, 51) have allowed studies on the mechanism of HCV entry and replication.

Viruses initiate infection by attaching to molecules or receptors on the cell surface. Expression and localization of these receptors are often important determinants of a cell's susceptibility to infection and of virus tropism for particular tissues. The observation that HCVpp only infect human liver-derived cell lines in vitro suggests that liver-specific receptors contribute to defining the hepatotropism of HCV. Current evidence suggests that at least three host cell molecules are important for HCV entry in vitro, i.e., the tetraspanin CD81 (5, 25, 35), scavenger receptor class B member I (SR-BI) (5, 23, 26, 39), and tight-junction (TJ) protein claudin 1 (CLDN1) (19). Recent data suggest that CLDN6 and CLDN9 can also function as coreceptors allowing HCV entry (33, 50). HCV glycoproteins (gps) have been reported to interact directly with CD81 and SR-BI (reviewed in reference 11). Mutagenesis and antibody-blocking studies with tagged versions of CLDN1 suggest that the first extracellular loop defines the interaction with HCV (19); however, the exact role(s) played by each of the receptors is unclear.

* Corresponding author. Mailing address: Division of Immunity and Infection, Institute for Biomedical Research, University of Birmingham, Vincent Drive, Birmingham B15 2TT, United Kingdom. Phone: (44) 121 414 8174. Fax: (44) 121 414 3599. E-mail: p.balfe@bham.ac.uk.

▽ Published ahead of print on 24 October 2007.

CD81 is expressed in most tissues and has been reported to localize to the basolateral surface of polarized epithelial cell lines (49). SR-BI is expressed within steroidogenic tissue, macrophages, and the liver (28), localizing to the apical and basolateral surfaces of Caco-2 epithelial cells (9). CLDN1 is a member of the integral membrane protein family, which is involved in the formation of TJ barrier function and is highly expressed in the liver (21).

TJs are continuous intercellular contacts at the apical poles of lateral cell membranes, appearing by electron microscopy as a series of discrete contacts between the plasma membranes of adjacent cells. TJs form a barrier which regulates the paracellular transit of solutes across an epithelium and are essential for establishing cell polarity by separating the apical and basolateral domains of epithelial cells (42). A number of proteins are found at TJs; most of them, like zonula occludens 1 (ZO-1), are peripheral membrane proteins associated with the cytoplasmic face of the junctional membrane. The members of the CLDN family of transmembrane proteins extend into the paracellular space, where they form homo- and heteroassociations with CLDNs on apposing cells (22). Many tissues in the body contain polarized cells, and hepatocytes within the liver are known to be highly polarized, with TJs separating the basolateral (sinusoidal) and apical (canalicular) domains. Hepatic polarity is critical to the functioning of the liver, with particular membrane domains performing specific tasks, such as biliary secretion from the canaliculi and serum protein secretion from the sinusoidal surface(s).

In order to initiate infection, many pathogens must breach the epithelial barrier to gain access to the body, and TJs are important in the natural defense against infection. The poor efficacy with which viral vectors deliver therapeutic genes to the airway epithelium highlighted the role of TJs in the resistance of epithelia to viral infection (34, 47). Several pathogen-encoded proteins are reported to disrupt junctional integrity to facilitate access to the host. *Clostridium perfringens* enterotoxin

removes CLDN3 and CLDN4 from TJs to promote bacterial invasion (41); *Helicobacter pylori* CagA protein disassembles the TJ proteins ZO-1 and junction adhesion molecule, leading to alterations in the apical-TJ complex during bacterial entry (3); and adenovirus-encoded fiber protein transiently disrupts TJ integrity during virus release (46). The recent identification of CLDN1 as a critical factor for HCV internalization (19) highlighted the importance of studying the role(s) of TJ formation and cell polarization in HCV entry. We demonstrate that the polarized colorectal adenocarcinoma Caco-2 cell line supports HCV infection. HCVpp infection and E1E2 gp interaction occurred predominantly via the apical surface of polarized Caco-2 cells. Disruption of TJs significantly increased viral entry, supporting a model where TJs impose a physical barrier by reducing viral access to receptors expressed on the lateral and basolateral cellular domains.

MATERIALS AND METHODS

Cell culture. Caco-2 and Huh-7.5 cells were maintained in Dulbecco's modified Eagle's medium supplemented with 10% fetal bovine serum (FBS) and 1% nonessential amino acids at 37°C in 5% CO_2. Caco-2 and T84 cells were kindly provided by Chris Tselepis (University of Birmingham, Birmingham, United Kingdom), and Huh-7.5 cells were kindly provided by Charles Rice (Rockefeller University, New York, NY). We seeded Caco-2 cells at 2×10^4 to 4×10^4 cells/cm^2 and Huh-7.5 cells at 1.5×10^4 to 3×10^4 cells/cm^2 on plastic, glass coverslips, or Transwell permeable PET membranes (0.4-μm pore size; BD Falcon), depending on the assay being performed. Caco-2 cells reached confluence 2 to 3 days after seeding, and monolayers were propagated for a further 6 days, with fresh medium being added every 3 days.

Measurement of dextran permeability. Paracellular permeability was quantified by measuring the transepithelial flux of a 4-kDa fluorescein isothiocyanate (FITC)-labeled dextran molecule (Sigma-Aldrich, Poole, Dorset, United Kingdom). Briefly, Caco-2 or Huh-7.5 cell monolayers were grown on 0.4-μm-pore-size Transwell PET membranes (0.33 cm^2) before the application of 200 μg of FITC-labeled dextran to the apical side of the monolayer. After incubation at 37°C for 3 h, a 200-μl aliquot of the medium was removed from the basolateral chamber and FITC-dextran fluorescence was measured (Aminco-Bowman series 2 luminescence spectrophotometer). For measurement of dextran flux in calcium-depleted monolayers, Caco-2 cells were treated with calcium-free medium (Minimum Essential Medium Eagle Spinner Modification [Sigma] plus 3% FBS, 1% nonessential amino acids, and 2 mM L-glutamate) supplemented with 0.5 mM EGTA for 16 h before application of the FITC-dextran.

Confocal microscopy. Caco-2 and Huh-7.5 cells were grown on 13-mm-diameter borosilicate glass coverslips (Fisher Scientific UK, Loughborough, United Kingdom) or 0.4-μm-pore-size Transwell PET membranes to the level of confluence required and fixed in 3% paraformaldehyde (for anti-CD81 monoclonal antibody [MAb] M38) or 100% ice-cold methanol (for all other antibodies). Cells were permeabilized for 30 min in 0.05% saponin–0.5% bovine serum albumin (BSA) in phosphate-buffered saline (PBS) and incubated with the primary antibodies anti-CD81 (M38) at 1:20 (F. Berditchevski, University of Birmingham, Birmingham, United Kingdom), anti-SR-BI (anti-ClaI) at 1:500 (BD Biosciences), anti-CLDN1 at 1:1,000 (Abnova), anti-occludin 1 at 1:1,000 (Zymed, Invitrogen), anti-ZO-1 at 1:1,000 (Zymed, Invitrogen), anti-epithelial cadherin (E-cadherin) at 1:1,000 (Zymed, Invitrogen), and anti-CD26 at 1:200 (Abcam, Cambridge, United Kingdom) for 1 h at room temperature in PBS-saponin-BSA. Cells were washed three times in PBS-saponin-BSA before the addition of a goat anti-mouse secondary antibody (Alexa 488; Invitrogen) at a 1:1,000 dilution in PBS-saponin-BSA and incubation for 1 h at room temperature. Cells were washed three times in PBS-saponin-BSA before counterstaining with 4′,6′-diamidino-2-phenylindole (DAPI; Invitrogen) in PBS for 5 min. Coverslips and PET membranes were mounted on glass slides (ProLong Gold antifade; Invitrogen). Laser scanning confocal microscopy was performed with a Zeiss Meta Head confocal microscope with a 63× water immersion objective. *x-y* sections were collected by Kalman averaging of four to eight images with *z* series collected by using a 0.76-μm optical slice. Linear plot image analysis of *x-y* sections was performed on a minimum of 10 cells, taking measurements for the plasma membrane and cytoplasm along a linear line plot. Calcium-depleted cells were stained in the same manner as nondepleted cells.

HCVpp generation and infection. Pseudoviruses were generated by transfecting 293T cells (American Type Culture Collection, Manassas, VA) with plasmids encoding human immunodeficiency virus (HIV) provirus expressing luciferase and HCV E1E2 strain H77, murine leukemia virus (MLV) envelope, vesicular stomatitis virus (VSV) G gp, or a no-envelope control, as previously described (25). Supernatants were harvested at 48 h posttransfection, pooled, clarified, and filtered. Virus containing medium was added to target cells plated as described above and incubated for 8 h, unbound virus was removed, and the medium was replaced with Dulbecco's modified Eagle's medium containing 3% FBS. At 96 h postinfection, the medium was removed and cells were lysed with cell lysis buffer (Promega, Madison, WI). Luciferase activity was assayed by the addition of luciferase substrate and measured for 10 s in a luminometer (Lumat LB 9507). Viral specific infectivity was expressed as the ratio of viral infectivity to Env$^-$ particle infectivity. Specific infectivities greater than 3 were considered significant based on previous infection data obtained with nonpermissive cells (25). In experiments to neutralize HCVpp entry, virus was incubated with anti-E2 antibodies 9/27 and 11/20 for 1 h at 37°C prior to incubation with target cells. The control anti-HIV gp120 antibody 10/76b was used in the same manner. For studying the effects of calcium depletion on HCVpp entry, cells were depleted of calcium for 16 h before the application of pseudotypes as described above.

HCVcc generation and infection. HCVcc strain JFH-1 was generated as previously described (30, 45). Briefly, RNA was transcribed in vitro from full-length genomes by using the Megascript T7 kit (Ambion) and electroporated into Huh-7.5 cells. At 72 and 96 h postelectroporation, supernatants were collected, pooled, and stored immediately at −80°C. Virus-containing medium was added to target cells plated as described above and incubated for 96 h at 37°C. Infected cells were detected by methanol fixation and staining for NS5A with anti-NS5A MAb 9E10 and Alexa 488-conjugated anti-mouse immunoglobulin G (IgG; Invitrogen). Infection was quantified by enumerating NS5A$^+$ cells and was defined as the number of infected cells or infectious units per milliliter. Cells from duplicate infections were collected by trypsinization, and RNA was prepared for quantitative reverse transcription-PCR (qRT-PCR) (RNeasy; QIAGEN).

Recombinant E1E2 binding. Caco-2 cells were grown on 0.4-μm-pore-size Transwell PET membranes until confluent and were allowed to polarize for 6 days. HCV strain HCV-1 (genotype 1a) E1E2 was expressed in CHO cells and purified as previously described (10) and was a kind gift of Jang Han (Novartis Vaccines, Emeryville, CA). HCV-1 E1E2 at 3 μg/ml in PBS was added to the apical or basal surface of polarized Caco-2 cells and incubated for 1 h at 37°C. Unbound antigen was removed by washing three times in PBS-BSA, and the cells were immediately fixed in ice-cold methanol. Bound antigen was visualized with a mixture of anti-E2 MAbs 9/75 and 7/59 at 1 μg/ml in PBS-BSA and anti-rat Ig-Alexa 633 (Invitrogen, CA). Cells were washed three times in PBS-BSA and counterstained with DAPI for 5 min. Transwell membranes were mounted on glass slides and imaged with a Zeiss Meta Head confocal microscope.

qRT-PCR. Purified cellular RNA samples were amplified for CD81, SR-BI, CLDN1, CLDN6, and CLDN9 with commercial quantification kits (ABI) in a single-tube RT-PCR in accordance with the manufacturer's guidelines (Cells-Direct kit; Invitrogen), and fluorescence was monitored in a 7900 HT real-time PCR machine (ABI). HCV amplification was performed by a modification of the method of Cook and colleagues (13, 43). In all reaction mixtures, the housekeeping gene for glyceraldehyde-3-phosphate dehydrogenase (GAPDH) was included as an internal endogenous control for amplification efficiency and RNA quantification (primer-limited endogenous control; ABI).

Statistical analysis. Results are expressed as the mean ± the standard error of the mean (SEM), except where stated to the contrary. Statistical analysis was performed by Student's *t* test, with $P < 0.05$ considered statistically significant.

RESULTS

Effect(s) of cell polarization on HCV receptor expression. To study the effect(s) of cell polarization on HCV receptor expression and function, we selected the human colon carcinoma cell line Caco-2, which is known to polarize in culture. We monitored polarization by assessing the permeability of cultures to the diffusion of FITC-labeled dextran (4 kDa) across cell membranes (barrier function) and the localization of CD26 (dipeptidyl-peptidase IV) to the apical cell surface (fence function). The majority of reports studying HCV entry use hepatoma cell lines, and so we investigated the ability of Huh-7.5 cells to establish a barrier to labeled-dextran flux.

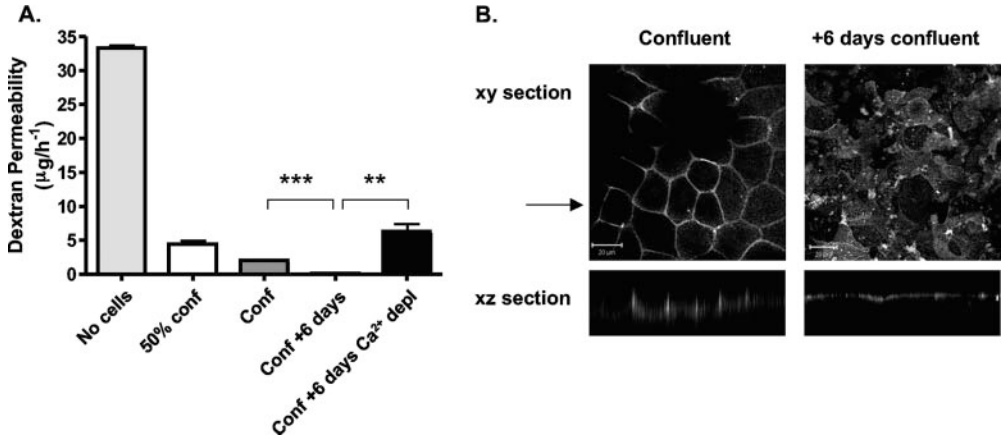

FIG. 1. Paracellular permeability and CD26 localization in Caco-2 cells. (A) Caco-2 cells were seeded onto 0.4-μm-pore-size Transwells to achieve different levels of cell confluence, i.e., a 50% confluent monolayer (50% conf), a confluent monolayer (Conf), and a confluent monolayer maintained for an additional 6 days (Conf + 6 days). At 16 h prior to the assay, duplicate Transwells (Conf + 6 days) were incubated in calcium-free medium plus 0.5 mM EGTA to disrupt TJs. FITC-dextran (4 kDa) was added to the medium in the upper reservoir on the apical side of the cell monolayer. After 3 h, aliquots of the basolateral medium were removed and the concentration of FITC-dextran was determined. The results show the mean ± SEM of triplicate samples for each condition. **, $P < 0.001$; ***, $P < 0.0001$ (*t* test). (B) Caco-2 cells were cultured on 0.4-μm-pore-size Transwells until confluent, fixed with methanol or cultured for an additional 6 days, and then fixed for antibody staining. Cells were stained with anti-CD26 antibody, and bound antibody was visualized with anti-mouse Ig-Alexa 488 secondary antibody and confocal microscopy. The large panels represent *x-y* sections, and the small panels are *x-z* sections, where the arrow indicates the plane the *z* section was taken from. *z* sections were compiled by taking 0.76-μm steps through each *x-y* section. The scale bars represent 20 μm.

Caco-2 and Huh-7.5 cells were propagated on 0.4-μm permeable filters, which allow access to medium by the apical and basolateral cellular domains. FITC-dextran was applied to the upper chamber, and the concentration in the lower chamber was measured over time. As TJ formation is dependent upon calcium and its depletion leads to the loss of TJ integrity, cells were depleted of calcium by propagation in calcium-free medium supplemented with 0.5 mM EGTA. In the absence of cells, the dextran flux rate was 34 $\mu g/h^{-1}$; this was reduced to 5 and 2.8 $\mu g/h^{-1}$ in the presence of subconfluent and confluent Caco-2 cell monolayers, respectively (Fig. 1A). Maintenance of confluent Caco-2 cells for 6 days resulted in a complete block of dextran flux that was abrogated by calcium depletion, confirming a barrier function (Fig. 1A). The reduced flow of dextran across subconfluent and confluent Caco-2 cell monolayers suggests that the cells provide a steric barrier to dextran movement and that cell monolayers require extended periods of culture to become fully polarized. In contrast, confluent Huh-7.5 cell monolayers allowed dextran to transit through the Transwell, with a negligible effect(s) of calcium depletion, suggesting that these cells were unable to exhibit a barrier function (data not shown).

CD26 is a cell surface ectopeptidase that localizes to the apical domain of polarized cells (16). Confluent monolayers of Caco-2 cells were propagated on 0.4-μm Transwell inserts and fixed immediately or cultured for an additional 6 days prior to fixation and stained for CD26 expression. Distinct patterns of CD26 staining were observed (Fig. 1B). In confluent cells, CD26 exhibited distinct membrane staining that localized to the lateral cell membranes (Fig. 1B). In contrast, after a further 6 days of culture, CD26 localized exclusively to the apical cell surface (Fig. 1B), confirming that Caco-2 cells form a polarized monolayer after extended culture.

We evaluated the mRNA levels of CD81, SR-BI, CLDN1, CLDN6, and CLDN9, proteins reported to be important for HCV entry, in polarized and nonpolarized Caco-2 cells by real-time qRT-PCR. As a control, we compared the mRNA levels to those present in Huh-7.5 cells. Comparable levels of CD81, SR-BI, CLDN1, and CLDN6 mRNAs were detected in all three samples; CLDN9 mRNA was not detected (Fig. 2). There was no discernible difference in the abundance of mRNAs measured between polarized and nonpolarized Caco-2 cells (Fig. 2). These data suggest that Caco-2 cells have the potential to express all of the molecules or viral receptors required for HCV entry.

HCV receptor and TJ protein expression was assessed in polarized and nonpolarized Caco-2 cells by laser scanning confocal microscopy. Caco-2 cells express CD81, SR-BI, and CLDN1, and protein levels increase with cell polarization

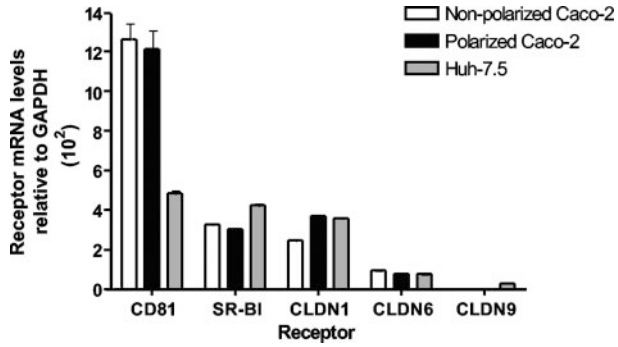

FIG. 2. HCV receptor mRNA levels in Caco-2 and Huh-7.5 cells. CD81, SR-BI, CLDN1, CLDN6, and CLDN9 mRNA levels in polarized (black) and nonpolarized Caco-2 (white) cells and Huh-7.5 cells (gray) were determined by real-time PCR. Data are expressed relative to the housekeeping gene for GAPDH (ΔCt).

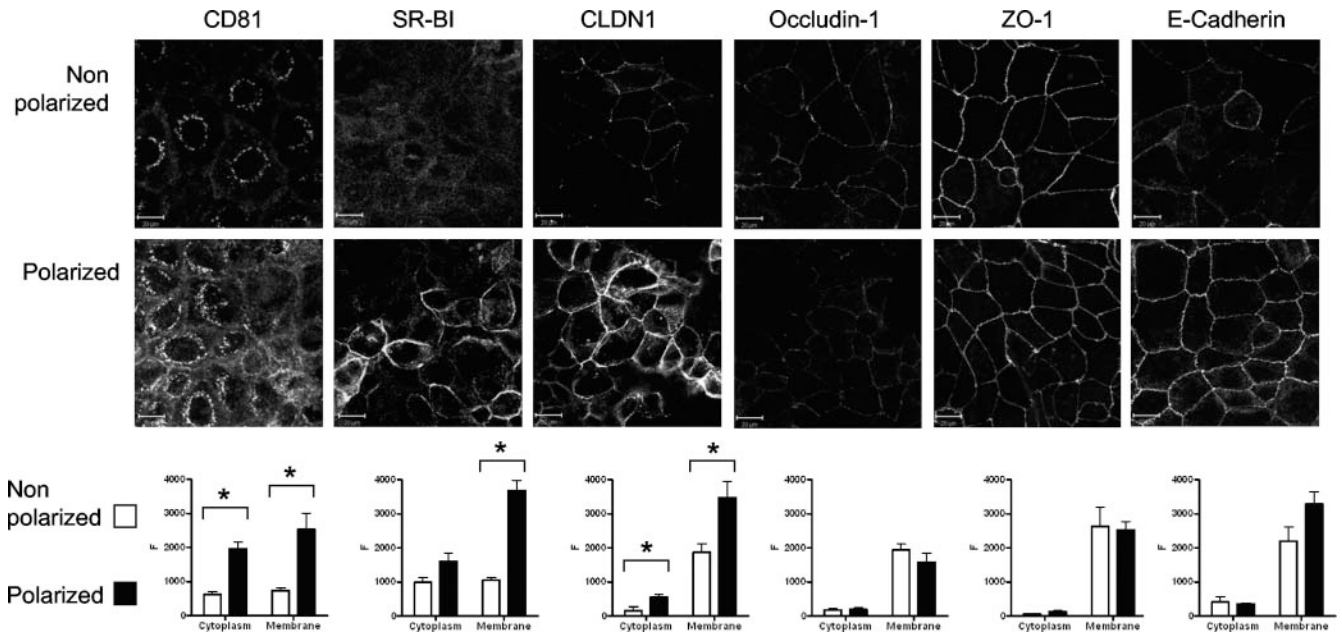

FIG. 3. HCV receptor and TJ protein expression in Caco-2 cells. Caco-2 cells were seeded onto glass coverslips under conditions necessary to achieve nonpolarized and polarized monolayers, as detailed in the legend to Fig. 1. Cells were stained with antibodies specific for CD81, SR-BI, CLDN1, occludin 1, ZO-1, or E-cadherin. Bound antibodies were visualized with an anti-mouse–Alexa 488 secondary antibody and confocal microscopy. Protein expression at the cytoplasm and plasma membrane was quantified with Zeiss LSM line plot analysis software, and data are expressed as arbitrary fluorescence units (F). Nonpolarized (white bars) and polarized (black bars) cells are shown, where the results reflect the mean ± SEM of at least 10 cells from each image. *, $P < 0.01$. The scale bars represent 20 μm.

(Fig. 3). Unfortunately, the only available anti-CLDN6 antibody failed to detect protein by indirect immunofluorescence, which may reflect the low affinity of the antibody or the low levels of endogenous CLDN6 within Caco-2 cells (data not shown). Quantitative analysis of receptor expression by linear fluorescent profiling of individual cells demonstrated a significant increase in intracellular and plasma membrane-expressed CD81 and SR-BI in polarized Caco-2 cells. CLDN1 was predominately expressed at the plasma membrane, and levels increased with polarization. In contrast, expression of the TJ proteins occludin 1 and ZO-1 did not alter with polarization. Similarly, expression of E-cadherin, a transmembrane protein with an important role in cell adhesion, did not alter with polarization (Fig. 3).

Plasma membrane-expressed CD81 demonstrated an apical pattern of staining in nonpolarized cells, which increased and redistributed to lateral cell-cell junctions with polarization (Fig. 4). SR-BI showed no evidence of reorganization upon polarization and localized predominantly to the lateral cell-cell junctions (Fig. 4). In nonpolarized Caco-2 cells, CLDN1 showed an apical location similar to that of ZO-1, consistent with the reported location of TJ structures (42), whereas in polarized cells CLDN1 localized to apical, lateral, and basolateral surfaces (Fig. 4). In summary, CD81, SR-BI, and CLDN1 protein expression is increased in polarized Caco-2 cells and CLDN1 relocalized from an apical site to apical, lateral, and basolateral surfaces.

Caco-2 cells support HCV entry and replication. To address whether Caco-2 cells support viral entry, we tested their ability to support HCVpp infection. As controls, we used the permissive Huh-7.5 hepatoma cell line and pseudoparticles expressing MLV and VSV G envelope gps, which infect most cell types. HCVpp-H77 infected nonpolarized and polarized Caco-2 cells with specific infectivities of 9.3 and 8.6, respectively (Fig. 5A), compared to 273.7 for Huh-7.5 cells (Fig. 5B). Normalization of HCVpp-H77 infectivity relative to MLVpp or VSVpp demonstrated that Caco-2 cells support HCVpp entry approximately 10-fold less than Huh-7.5 cells. However, this low-level infection was abrogated by incubating HCVpp with neutralizing anti-E2 MAbs 9/27 and 11/20, confirming a gp-dependent entry process (Fig. 5A). An irrelevant anti-HIV gp120 MAb, 10/76b, had no effect on HCVpp infection of Caco-2 or Huh-7.5 cells. MLVpp and VSVpp infected Caco-2 cells less efficiently when the cells were polarized, suggesting that the expression of both MLV and VSV receptors is modulated upon cell polarization or that NL4.3 promoter activity is suboptimal in polarized cells. Our experiments suggest that the HIV promoter long terminal repeat is reduced in polarized Caco-2 cells (data not shown), consistent with a report from Acheampong and colleagues (1). Normalization of HCVpp infection of polarized and nonpolarized Caco-2 cells relative to MLVpp or VSVpp demonstrated a nonsignificant two- to threefold increase in HCV gp-dependent entry in polarized Caco-2 cells.

HCVcc strain JFH-1 infected nonpolarized and polarized Caco-2 cells with infectivities of 177.5 and 107.0 IU/ml, compared to 5.8×10^6 IU/ml for Huh-7.5 cells (Fig. 5C and D). HCVcc infection of Caco-2 cells resulted in small foci of infected $NS5A^+$ cells, in comparison to the large foci observed in infected Huh-7.5 cells (Fig. 5C and D), which may partly reflect the low level of HCV-specific, gp-dependent entry observed in Caco-2 cells. In support of this interpretation, quantification of HCV RNA levels in JFH-1-infected Huh-7.5 and Caco-2 cells

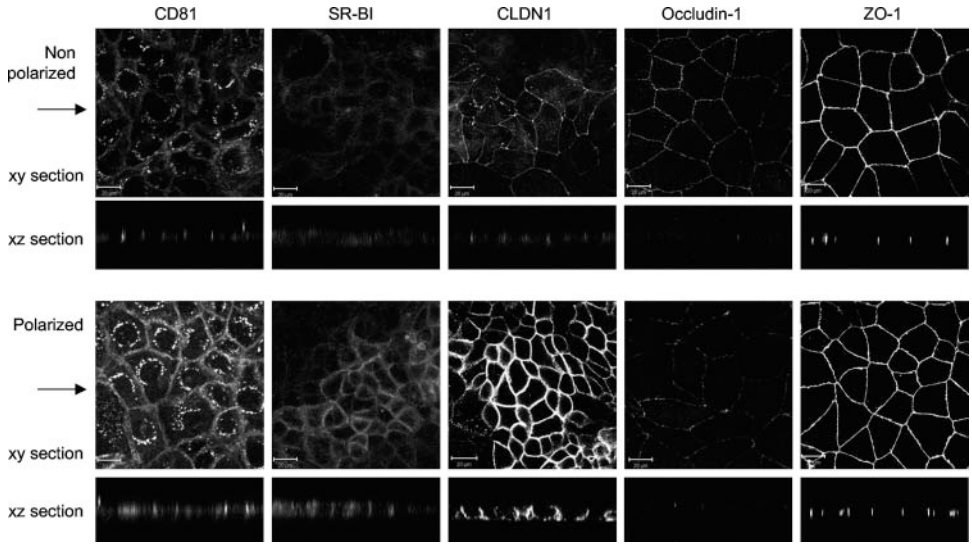

FIG. 4. HCV receptor and TJ protein localization. Caco-2 cells were seeded onto glass coverslips under conditions optimized to achieve nonpolarized and polarized monolayers, as detailed in the legend to Fig. 1. Cells were stained with antibodies specific for CD81, SR-BI, CLDN1, occludin 1, and ZO-1. Bound antibodies were visualized with an anti-mouse–Alexa 488 secondary antibody and confocal microscopy. The large panel represents *x-y* sections, and the small panel represents *x-z* sections taken from each of the corresponding *x-y* sections, with the arrow indicating the plane the *z* section was taken from. *z* sections were compiled by taking 0.76-μm steps through each *x-y* section. The scale bars represent 20 μm.

by RT-PCR showed comparable levels of HCV RNA per infected cell after normalization to the number of $NS5A^+$ cells (Fig. 5E). In summary, these data demonstrate that HCVpp and HCVcc infect nonpolarized and polarized Caco-2 cells with comparable efficiencies.

Polarized entry of HCVpp into Caco-2 cells. To investigate whether HCVpp infects Caco-2 cells via the apical or basolateral surface, the cells were grown on 0.4-μm-pore-size Transwell inserts to form polarized monolayers (Fig. 6A). By exposing only the apical or basolateral surface(s) to HCVpp, we were able to determine the preferred route(s) of entry into the cell. HCVpp-H77 entry was significantly higher via the apical surface compared to the basolateral surface (Fig. 6B). In contrast, VSVpp only infected polarized cells via the apical surface (Fig. 6B). To investigate whether polarized Caco-2 cells form an impermeable barrier to pseudoparticles, we added high-titer VSVpp to the apical or basolateral reservoir(s) for 8 h of incubation, collected medium from both chambers, and tested it for viral infectivity in a secondary independent infection of Huh-7.5 cells. We found that 99.6% of the viral infectivity remained in the applied reservoir, with no evidence of transport across the polarized monolayer (Fig. 6C), confirming that virus applied to the apical or basolateral surface had minimal access to the opposing polar surface.

To further investigate the mechanism(s) underlying the preferred apical route of HCVpp entry into polarized Caco-2 cells, we used recombinant HCV E1E2 gps as a tool to study virus-receptor interactions. HCV-1 E1E2 binds specifically to CHO cells transduced to express human CD81 or human SR-BI, and we have identified anti-E2 MAbs that can specifically recognize E1E2 bound to cells via CD81 (MAb 9/27) or SR-BI (MAb 7/59) (23, 29). Caco-2 cells were grown on 0.4-μm Transwells until polarized, and the apical or basolateral surfaces were incubated with HCV-1 E1E2 for 1 h at 37°C. Bound gps were visualized with a cocktail of anti-E2 MAbs 9/27 and 7/59, anti-rat Ig-Alexa 488, and confocal imaging. E1E2 preferentially bound to the apical surface, with no discernible signal in the absence of gps (Fig. 6D). Quantification of cell-bound anti-E2 MAbs confirmed a significantly higher level of E1E2 binding to the apical surface compared to the basolateral domain (Fig. 6D).

All three viral receptors were predominantly located at the lateral cell-cell junctions in polarized cells, suggesting that this pool of receptors may be inaccessible to HCV in fully polarized cells. To test this hypothesis, we depolarized Caco-2 cells by depleting calcium and assessed their ability to support HCVpp and HCVcc infection. After virus inoculation, the cells were refed calcium-containing medium to restore TJ formation. Depletion of polarized Caco-2 cells of calcium led to a 10-fold increase in HCVpp-H77 infection but had a negligible effect on VSVpp infection (Fig. 7A). In contrast, depleting confluent cultures of Huh-7.5 cells of calcium had no effect on HCVpp or VSVpp infection (Fig. 7B), consistent with their inability to form TJs. Similarly, disruption of TJs led to a modest 2.2-fold increase in JFH-1 infection of polarized Caco-2 cells but had a minimal effect on Huh-7.5 cell permissivity (Fig. 7C). Calcium depletion of polarized Caco-2 cells led to redistribution of CD81, SR-BI, and CLDN1, with all receptors showing ubiquitous expression at cell surfaces and increased levels of intracellular CLDN1 and occludin 1 (Fig. 7D). Depletion of Huh-7.5 cells of calcium produced no perturbation in CD81 or SR-BI localization, but both CLDN1 and occludin 1 demonstrated fragmented expression at the plasma membrane (Fig. 7E). Depletion of JFH-1-infected polarized Caco-2 cells of calcium did not promote HCVcc spreading, suggesting that TJ formation was not directly responsible for the nonspreading phenotype (data not shown). These data demonstrate that HCV gps and particles preferentially interact with the apical

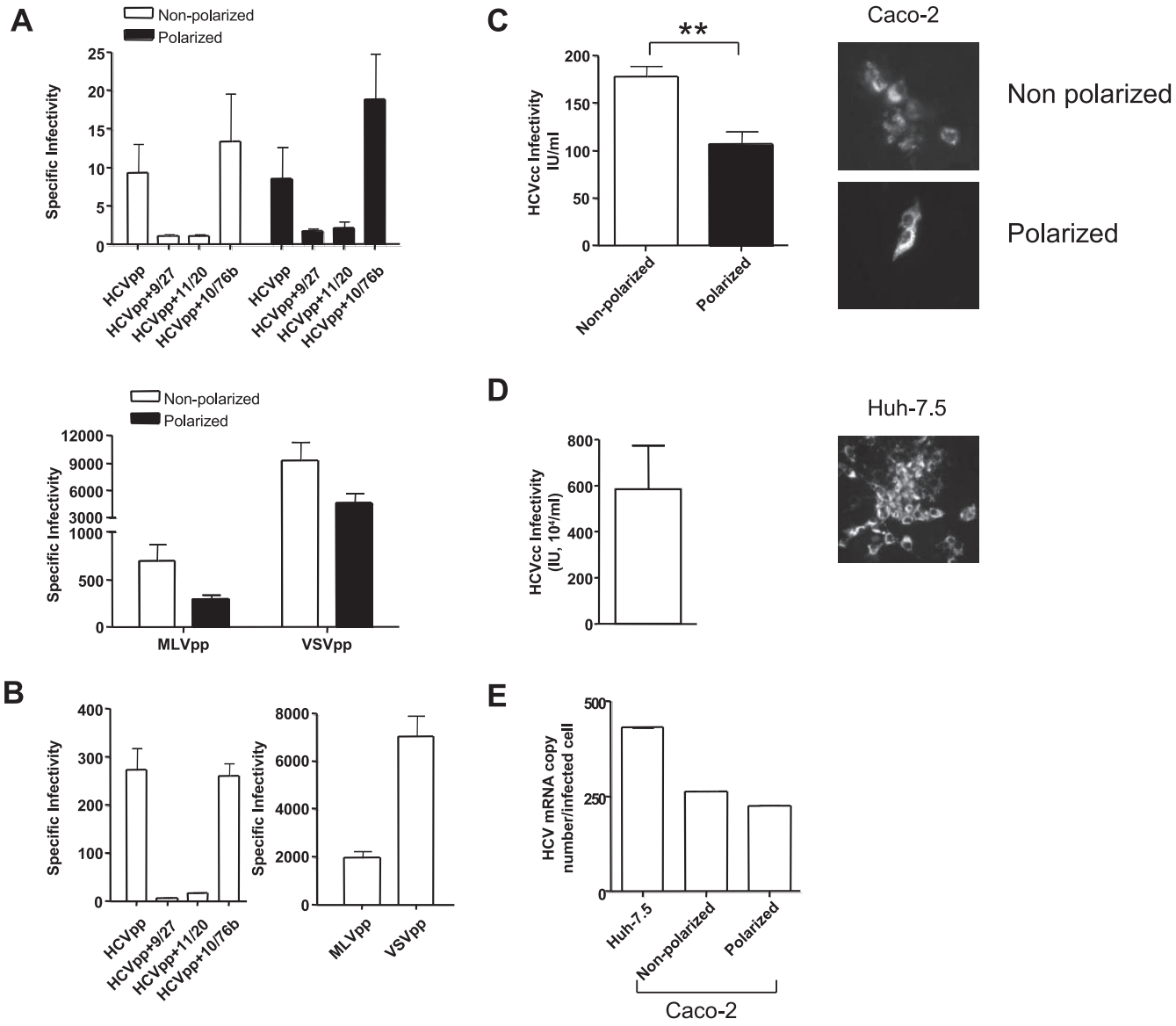

FIG. 5. HCV entry and infection of polarized cells. (A) HCVpp infection of nonpolarized (white bars) or polarized (black bars) Caco-2 cells in the presence or absence of neutralizing anti-HCV E2 MAbs 9/27 and 11/20 and control anti-HIV gp120 MAb 10/76b. MLVpp and VSVpp infection of nonpolarized (white bars) or polarized (black bars) Caco-2 cells is shown. Data are expressed as specific infectivity where the ratio of luciferase activity for HCVpp or control MLV/VSVpp to Env^- particles is shown. (B) HCVpp, MLVpp, and VSVpp infection of Huh-7.5 hepatoma cells seeded under conditions optimized for infection (see Materials and Methods). (C) HCVcc JFH-1 infection of nonpolarized (white bar) and polarized (black bar) Caco-2 cells. (D) HCVcc JFH-1 infection of Huh-7.5 hepatoma cells. Infected cells were visualized after 96 h by staining for NS5A expression, and the number of infected cells was defined as the number of infectious units per milliliter. (E) HCV copy numbers in JFH-1-infected Caco-2 and Huh-7.5 cells were determined by real-time PCR with an endogenous control (the gene for GAPDH) to quantify the HCV copy number relative to cellular RNA (ΔCt). HCV RNA levels were normalized to the number of $NS5A^+$ cells. **, $P < 0.001$ (t test).

surface of polarized Caco-2 cells and that disruption of TJs increases HCV entry, consistent with increased receptor accessibility after TJ disruption.

DISCUSSION

The recent identification of CLDNs as critical factors important for HCV internalization highlighted the importance of studying the effect(s) of TJ formation and cell polarization on HCV entry (19, 50). We demonstrate here that HCV infects nonpolarized and polarized Caco-2 cells, suggesting that CLDN receptor activity may be independent of its TJ function (Fig. 4). However, comparing the abilities of nonpolarized and polarized cells to support HCV entry is complicated by several observations. Firstly, CD81, SR-BI, and CLDN1 expression levels increase with cell polarization (Fig. 3); secondly, CLDN1 localization differs between nonpolarized and polarized cells (Fig. 4); and thirdly, polarized Caco-2 cells demonstrate a reduced capacity to transcribe and translate proviral genomes, modulating the activity of the reporter genes used in the pseu-

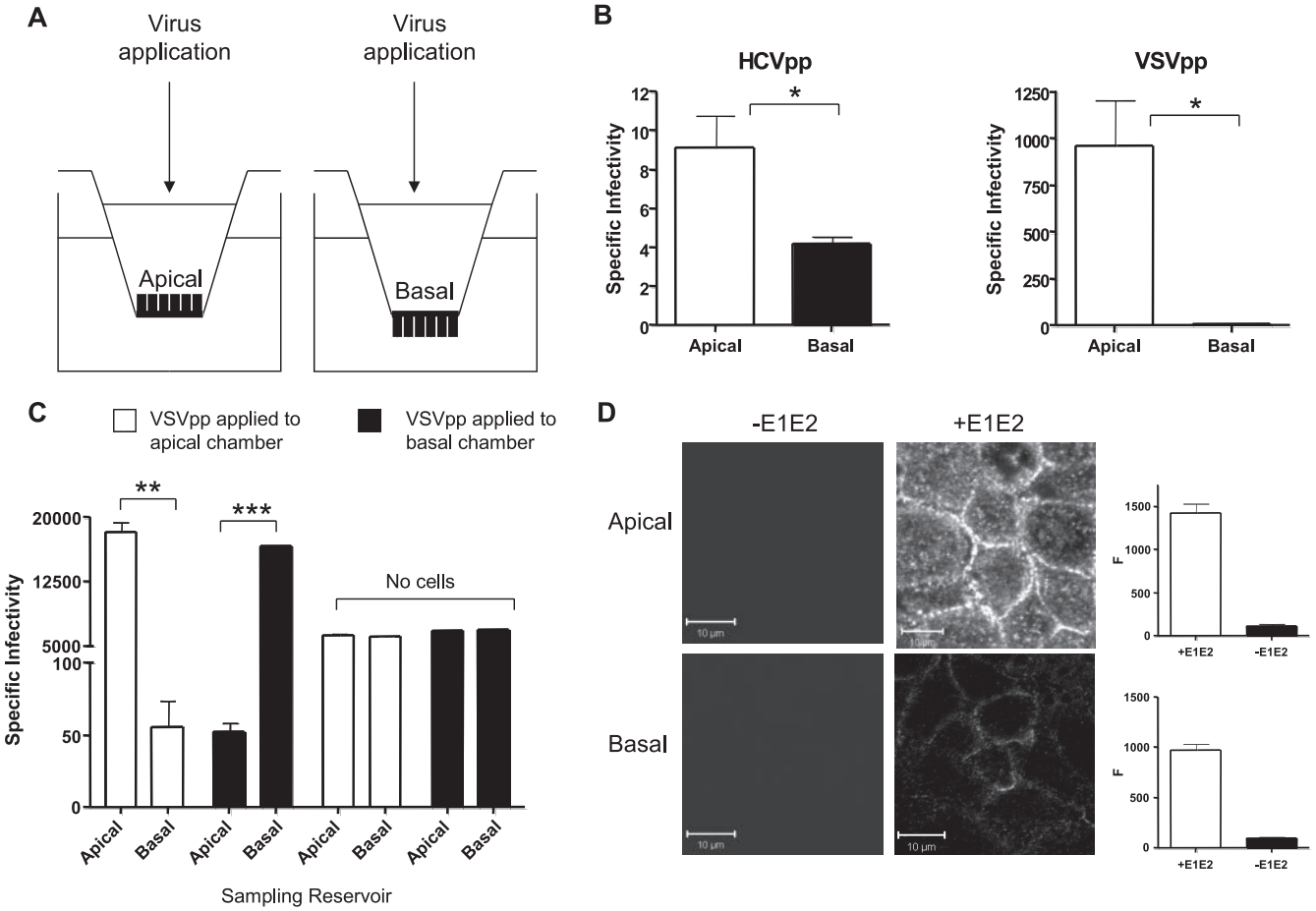

FIG. 6. Effect of polarity on HCVpp infection. (A) Caco-2 cells were grown until polarized on 0.4-μm-pore-size Transwell inserts, allowing access to the apical or basal membrane for HCVpp or VSVpp infection. (B) HCVpp and VSVpp infection of polarized Caco-2 cells via the apical or basal surface. Data are expressed as specific infectivity where the ratio of luciferase activity for HCVpp or control VSVpp to Env$^-$ particles is shown. (C) To control for virus mixing between the apical and basal compartments, the medium was removed from both reservoirs after an 8-h VSVpp infection and infectivity was assessed by inoculating Huh-7.5 cells. As a control, VSVpp was applied to the upper and lower reservoirs of Transwells with no cells. Ninety-six percent of the VSVpp applied to the apical surface of polarized Caco-2 cells (white bars) remained in the apical reservoir. The result was similar when virus was applied to the basal reservoir (black bars). In the absence of cells, infectious VSVpp were found equally distributed between the upper and lower chambers. (D). HCV strain HCV-1 E1E2 was applied to the apical or basal surface of polarized Caco-2 cells at 3 μg/ml in PBS and incubated for 1 h at 37°C. Unbound antigen was removed by washing, and the cells were fixed with ice-cold methanol. Bound antigen was visualized with rat anti-E2 MAbs 9/75 and 7/59, anti-rat–Alexa 633, and confocal microscopy. Bound MAbs were quantified with Zeiss LSM line plot software, and the data are expressed as arbitrary fluorescence units (F). The upper and lower parts of the panel show the binding of E1E2 when applied to the apical or basal surface, respectively. The scale bars represent 10 μm. **, $P < 0.001$; ***, $P < 0.0001$.

doparticle system (1). Recent reports studying the relationship between receptor density and HCV infection (2, 23, 27) suggest that the increased levels of CD81 and SR-BI observed in polarized Caco-2 cells would promote viral entry. However, any receptor-dependent increase in HCVpp entry into polarized cells may be offset by the reduced transcription and/or translation of the lentiviral vector postentry, as evinced by the reduced infectivity of MLVpp and VSVpp for polarized cells (Fig. 5). If one normalizes HCVpp infection of nonpolarized and polarized Caco-2 cells to MLVpp or VSVpp infectivity, there is a modest two- to threefold increase in HCVpp infection of polarized cells that is not significant (Fig. 5).

CD81, SR-BI, and CLDN1 protein levels increase in polarized Caco-2 cells (Fig. 3). Similar increases in receptor expression levels were noted in Huh-7.5 cells at high cell density, suggesting that factors regulating protein expression may be independent of TJ formation (Anne Schwarz, unpublished data). The recent report that CLDN6 and CLDN9 can function as coreceptors for HCV prompted us to investigate their expression in Caco-2 cells. CLDN1 and CLDN6 mRNAs were detected in Caco-2 cells and control Huh-7.5 cells, raising questions as to which CLDN family member is used by HCV to gain entry into cells (Fig. 2). This may be further complicated by the ability of CLDNs to form heterotypic oligomers (17). In the absence of antibodies that can reliably detect endogenous levels of CLDN6, we are unable to investigate the CLDN dependence of HCV infection of Caco-2 cells.

HCVpp preferentially infected polarized Caco-2 cells via the apical surface compared to the basolateral domain (Fig. 6A). The increased binding of recombinant HCV E1E2 gps to the apical surface (Fig. 6D) suggests greater expression of functional receptors in the apical domain. However, CD81, SR-BI,

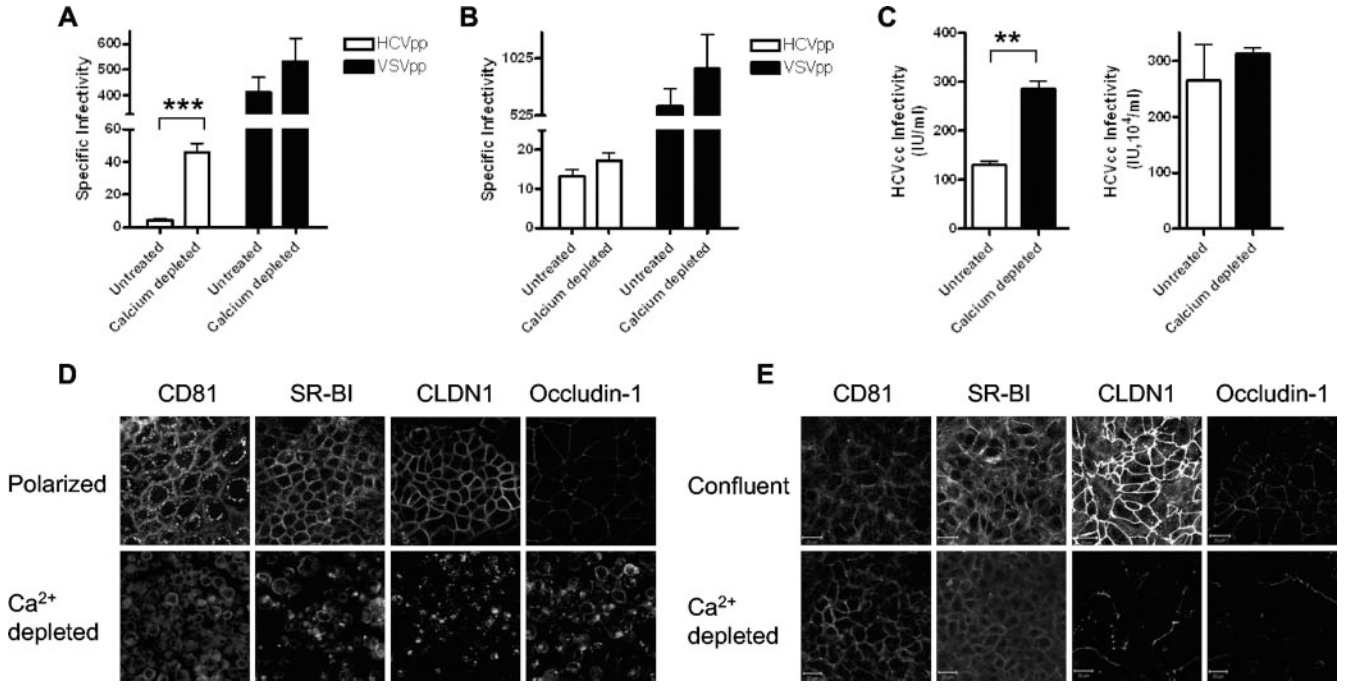

FIG. 7. Effect of disrupting TJs on HCV entry and infection. (A) Caco-2 cells were grown until polarized. To investigate the effect of disrupting TJs on HCV entry, cells were depleted of calcium by incubation with calcium-free medium supplemented with 0.5 mM EGTA for 16 h. Treated and untreated cells were tested for the ability to support infection with HCVpp (white bars) or VSVpp (black bars). (B) Untreated and calcium-depleted Huh-7.5 cells were tested for the ability to support infection with HCVpp (white bars) or VSVpp (black bars). Data are expressed as specific infectivity where the ratio of luciferase activity for HCVpp or control VSVpp to Env^- particles is shown. (C) Effect of depleting polarized Caco-2 (left side) and Huh-7.5 (right side) cells of calcium on JFH-1 infectivity. Infected cells were visualized after 96 h by staining for NS5A expression, and the number of infected cells was defined as the number of infectious units per milliliter. Confocal imaging of CD81, SR-BI, CLDN1, and occludin 1 in untreated polarized and depleted Caco-2 (D) and nonpolarized Huh-7.5 (E) cells. The scale bars represent 20 μm. **, $P < 0.001$; ***, $P < 0.0001$.

and CLDN1 are not solely expressed at the apical surface in polarized cells. CLDN1 relocalized from the apical pole of the lateral cell membrane to the lateral cell-cell junction and basolateral domains in polarized Caco-2 cells, whereas the expression and localization of the TJ proteins ZO-1 and occludin 1 were unchanged (Fig. 4). Since there is no obvious pattern of increased receptor staining at the apical surface compared to the basolateral region, there are several explanations for the data. Firstly, simple visualization of receptor molecules may not define function and more detailed methods of studying receptor associations may be required (24); secondly, additional molecules not studied in this report may define apical receptor activity; or thirdly, TJs within polarized cells may form a physical barrier preventing virus access to receptors at the lateral cell-cell junctions. The latter interpretation is supported by data showing that depleting polarized Caco-2 cells of calcium increased paracellular transit (Fig. 1A) and significantly increased HCVpp and HCVcc infection (Fig. 7). In contrast, depleting Huh-7.5 cells of calcium had no effect on HCVpp or HCVcc infectivity, consistent with our observation that these cells do not form TJ-dependent paracellular barriers.

Many viruses exhibit polarized routes of entry into primary and transformed epithelial cells, including vaccinia virus (37), VSV (8, 20, 40), human cytomegalovirus (18), Crimean-Congo hemorrhagic fever virus (12), coxsackievirus B, and adenovirus (14, 15). Polarized entry can be mediated by several mechanisms, such as differential distribution of viral receptors on apical and basolateral surfaces, inaccessibility or inactivation of viral receptors, and postentry factors inhibiting viral replication. The literature on VSV entry is controversial, with an early report demonstrating basolateral infection of MDCK cells (20) and more recent reports of the virus infecting airway epithelial and Caco-2 cells via the apical surface (8, 40). This variation may reflect differences in the origin of the airway cells, culture conditions, and/or degree of polarization. Our data are consistent with the latter reports, demonstrating VSVpp infection of Caco-2 cells via the apical surface (8, 40).

Caco-2 cells support a low level of HCV infection with limited evidence of cell-cell spreading, as demonstrated by the small number of $NS5A^+$-infected cells within a focus compared to infected Huh-7.5 cells (Fig. 5C). Focus size reflects the efficiency of viral spreading by cell-free and cell-cell routes, with cells at high density favoring the latter route (44). Disruption of TJs in JFH-1-infected Caco-2 cells had no effect on viral spreading. Preliminary data demonstrate that JFH-1 does not infect Caco-2 cells by direct cell-cell transfer, implying that Caco-2 cells are defective in the cellular pathways required for this route of infection and suggesting an explanation for the small focus size (Jennifer Timpe, unpublished data).

The principal site of HCV replication is believed to be hepatocytes within the liver. Hepatocytes are highly polarized, with TJs separating their plasma membrane into apical-canalicular and basolateral-sinusoidal domains (48). We recently demonstrated that CLDN1 is expressed at the apical and basolateral

surfaces of hepatocytes in normal liver tissue (36), consistent with our findings on polarized Caco-2 cells. The ability of nonpolarized Caco-2 cells to support HCVpp entry (Fig. 5) suggests that functional TJ complexes are not required for viral receptor activity. Evans and colleagues (19) reported that a CLDN1 variant lacking the C-terminal region supported HCV entry into Huh-7.5 hepatoma cells. Since this region of CLDN1 mediates interactions with cytoplasmic and signaling components of the TJ complex (38), these data support a model where HCV may enter cells by using nonjunctional forms of CLDNs.

The observation that disrupting TJs in polarized Caco-2 cells increased HCV entry (Fig. 7) raises the important question of whether perturbation of hepatocellular TJs in the liver promotes HCV infection and replication in vivo. HCV is likely to enter the liver through the sinusoidal blood and initially have access to the basolateral form(s) of the receptors on hepatocytes. If the restricted HCVpp entry of polarized Caco-2 cells via the basolateral surface is an accurate model for polarized hepatocytes, HCV may preferentially target hepatocytes where cell-cell contacts are damaged, allowing greater access to receptors expressed at the lateral cell-cell junctions. It is noteworthy that following liver transplantation for late-stage HCV infection, where the liver graft may be injured during surgical procedures, viral infection of the allograft can result in high viral RNA loads and rapidly progressive disease (32). Reports detailing increased rates of fibrosis progression and reduced time to significant HCV-related disease in the transplanted population are consistent with an increased viral burden in the newly infected liver (6).

TJ proteins have been reported to act as receptors for a range of viruses, including the junctional adhesion molecule for reovirus (4) and feline calicivirus (31) and the coxsackievirus and adenovirus receptor for coxsackievirus and adenovirus (7). Recent work detailing the complex mechanism(s) underlying adenovirus entry and the use of decay-accelerating factor to promote virus interaction(s) with TJ-associated coxsackievirus and adenovirus receptor highlight the dynamic properties of the intercellular junctions (15). We demonstrate that HCV can infect Caco-2 cells and that entry occurs independently of TJ formation. HCVpp infection and E1E2 gp interaction with polarized Caco-2 cells occur predominantly via the apical surface; however, disruption of TJs increases viral entry. These data support a model where TJs provide a physical barrier to infection by reducing viral access to receptors expressed in the lateral and basolateral cellular domains. It is interesting to speculate whether sites of CD81, SR-BI, and CLDN1/6/9 expression pose a barrier to HCV infection in vivo. Future experiments will investigate whether HCV infection influences TJ function and cell polarity.

ACKNOWLEDGMENTS

We thank T. Wakita for JFH-1, C. M. Rice for Huh-7.5 cells and anti-NS5A MAb 9E10, J. Han for HCV-1 E1E2 gps, F. Berditchevski for anti-CD81 MAb M38, C. Tselepis for Caco-2 cells, and H. Deng for CLDN expression constructs. We thank Jennifer Timpe and Zania Stamataki for reading the manuscript and providing comments.

This work was supported by PHS grant AI50798, MRC, and The Wellcome Trust.

REFERENCES

1. **Acheampong, E. A., Z. Parveen, L. W. Muthoga, V. Wasmuth-Peroud, M. Kalayeh, A. Bashir, R. Diecidue, M. Mukhtar, and R. J. Pomerantz.** 2005. Molecular interactions of human immunodeficiency virus type 1 with primary human oral keratinocytes. J. Virol. **79:**8440–8453.
2. **Akazawa, D., T. Date, K. Morikawa, A. Murayama, M. Miyamoto, M. Kaga, H. Barth, T. F. Baumert, J. Dubuisson, and T. Wakita.** 2007. CD81 expression is important for the permissiveness of Huh7 cell clones for heterogeneous hepatitis C virus infection. J. Virol. **81:**5036–5045.
3. **Amieva, M. R., R. Vogelmann, A. Covacci, L. S. Tompkins, W. J. Nelson, and S. Falkow.** 2003. Disruption of the epithelial apical-junctional complex by Helicobacter pylori CagA. Science **300:**1430–1434.
4. **Barton, E. S., J. C. Forrest, J. L. Connolly, J. D. Chappell, Y. Liu, F. J. Schnell, A. Nusrat, C. A. Parkos, and T. S. Dermody.** 2001. Junction adhesion molecule is a receptor for reovirus. Cell **104:**441–451.
5. **Bartosch, B., J. Dubuisson, and F. L. Cosset.** 2003. Infectious hepatitis C virus pseudo-particles containing functional E1-E2 envelope protein complexes. J. Exp. Med. **197:**633–642.
6. **Berenguer, M., V. Aguilera, M. Prieto, F. San Juan, J. M. Rayon, S. Benlloch, and J. Berenguer.** 2006. Significant improvement in the outcome of HCV-infected transplant recipients by avoiding rapid steroid tapering and potent induction immunosuppression. J. Hepatol. **44:**717–722.
7. **Bergelson, J. M., J. A. Cunningham, G. Droguett, E. A. Kurt-Jones, A. Krithivas, J. S. Hong, M. S. Horwitz, R. L. Crowell, and R. W. Finberg.** 1997. Isolation of a common receptor for coxsackie B viruses and adenoviruses 2 and 5. Science **275:**1320–1323.
8. **Borok, Z., J. E. Harboe-Schmidt, S. L. Brody, Y. You, B. Zhou, Li, X., P. M. Cannon, K. J. Kim, E. D. Crandall, and N. Kasahara.** 2001. Vesicular stomatitis virus G-pseudotyped lentivirus vectors mediate efficient apical transduction of polarized quiescent primary alveolar epithelial cells. J. Virol. **75:**11747–11754.
9. **Cai, S. F., R. J. Kirby, P. N. Howles, and D. Y. Hui.** 2001. Differentiation-dependent expression and localization of the class B type I scavenger receptor in intestine. J. Lipid Res. **42:**902–909.
10. **Choo, Q. L., G. Kuo, R. Ralston, A. Weiner, D. Chien, G. Van Nest, J. Han, K. Berger, K. Thudium, C. Kuo, et al.** 1994. Vaccination of chimpanzees against infection by the hepatitis C virus. Proc. Natl. Acad. Sci. USA **91:**1294–1298.
11. **Cocquerel, L., C. Voisset, and J. Dubuisson.** 2006. Hepatitis C virus entry: potential receptors and their biological functions. J. Gen. Virol. **87:**1075–1084.
12. **Connolly-Andersen, A. M., K. E. Magnusson, and A. Mirazimi.** 2007. Basolateral entry and release of Crimean-Congo hemorrhagic fever virus in polarized MDCK-1 cells. J. Virol. **81:**2158–2164.
13. **Cook, L., K.-W. Ng, A. Bagabag, L. Corey, and K. R. Jerome.** 2004. Use of the MagNA pure LC automated nucleic acid extraction system followed by real-time reverse transcription-PCR for ultrasensitive quantitation of hepatitis C virus RNA. J. Clin. Microbiol. **42:**4130–4136.
14. **Coyne, C. B., and J. M. Bergelson.** 2005. CAR: a virus receptor within the tight junction. Adv. Drug Delivery Rev. **57:**869–882.
15. **Coyne, C. B., and J. M. Bergelson.** 2006. Virus-induced Abl and Fyn kinase signals permit coxsackievirus entry through epithelial tight junctions. Cell **124:**119–131.
16. **Darmoul, D., M. Lacasa, L. Baricault, D. Marguet, C. Sapin, P. Trotot, A. Barbat, and G. Trugnan.** 1992. Dipeptidyl peptidase IV (CD 26) gene expression in enterocyte-like colon cancer cell lines HT-29 and Caco-2. Cloning of the complete human coding sequence and changes of dipeptidyl peptidase IV mRNA levels during cell differentiation. J. Biol. Chem. **267:**4824–4833.
17. **Daugherty, B. L., C. Ward, T. Smith, J. D. Ritzenthaler, and M. Koval.** 2007. Regulation of heterotypic claudin compatibility. J. Biol. Chem. **282:**30005–30013.
18. **Esclatine, A., M. Lemullois, A. L. Servin, A. M. Quero, and M. Geniteau-Legendre.** 2000. Human cytomegalovirus infects Caco-2 intestinal epithelial cells basolaterally regardless of the differentiation state. J. Virol. **74:**513–517.
19. **Evans, M. J., T. von Hahn, D. M. Tscherne, A. J. Syder, M. Panis, B. Wolk, T. Hatziioannou, J. A. McKeating, P. D. Bieniasz, and C. M. Rice.** 2007. Claudin-1 is a hepatitis C virus co-receptor required for a late step in entry. Nature **446:**801–805.
20. **Fuller, S., C.-H. von Bonsdorff, and K. Simons.** 1984. Vesicular stomatitis virus infects and matures only through the basolateral surface of the polarized epithelial cell line, MDCK. Cell **38:**65–77.
21. **Furuse, M., K. Fujita, T. Hiiragi, K. Fujimoto, and S. Tsukita.** 1998. Claudin-1 and -2: novel integral membrane proteins localizing at tight junctions with no sequence similarity to occludin. J. Cell Biol. **141:**1539–1550.
22. **Furuse, M., H. Sasaki, and S. Tsukita.** 1999. Manner of interaction of heterogeneous claudin species within and between tight junction strands. J. Cell Biol. **147:**891–903.
23. **Grove, J., T. Huby, Z. Stamataki, T. Vanwolleghem, P. Meuleman, M. Farquhar, A. Schwarz, M. Moreau, J. S. Owen, G. Leroux-Roels, P. Balfe, and J. A. McKeating.**

2007. Scavenger receptor BI and BII expression levels modulate hepatitis C virus infectivity. J. Virol. **81:**3162–3169.
24. **Harris, H. J., G. M. Reynolds, M. J. Farquhar, C. J. Mee, A. E. Jennings, K. Hu, P. Lalor, D. H. Adams, P. Balfe, S. Hubscher, and J. A. McKeating.** 2007. Hepatitis C virus receptor localization in normal and diseased liver tissue, abstr. O-1. *In* 14th International Symposium on Hepatitis C Virus and Related Viruses.
25. **Hsu, M., J. Zhang, M. Flint, C. Logvinoff, C. Cheng-Mayer, C. M. Rice, and J. A. McKeating.** 2003. Hepatitis C virus glycoproteins mediate pH-dependent cell entry of pseudotyped retroviral particles. Proc. Natl. Acad. Sci. USA **100:**7271–7276.
26. **Kapadia, S. B., H. Barth, T. Baumert, J. A. McKeating, and F. V. Chisari.** 2007. Initiation of hepatitis C virus infection is dependent on cholesterol and cooperativity between CD81 and scavenger receptor B type I. J. Virol. **81:**374–383.
27. **Koutsoudakis, G., E. Herrmann, S. Kallis, R. Bartenschlager, and T. Pietschmann.** 2007. The level of CD81 cell surface expression is a key determinant for productive entry of hepatitis C virus into host cells. J. Virol. **81:**588–598.
28. **Krieger, M.** 2001. Scavenger receptor class B type I is a multiligand HDL receptor that influences diverse physiological systems. J. Clin. Investig. **108:** 793–797.
29. **Lai, W., P. Sun, J. Zhang, A. Jennings, P. Lalor, S. Hubscher, J. McKeating, and D. Adams.** 2006. Expression of DC-SIGN and DC-SIGNR on human sinusoidal endothelium: a role for capturing hepatitis C virus particles. Am. J. Pathol. **169:**200–208.
30. **Lindenbach, B. D., M. J. Evans, A. J. Syder, B. Wolk, T. L. Tellinghuisen, C. C. Liu, T. Maruyama, R. O. Hynes, D. R. Burton, J. A. McKeating, and C. M. Rice.** 2005. Complete replication of hepatitis C virus in cell culture. Science **309:**623–626.
31. **Makino, A., M. Shimojima, T. Miyazawa, K. Kato, Y. Tohya, and H. Akashi.** 2006. Junctional adhesion molecule 1 is a functional receptor for feline calicivirus. J. Virol. **80:**4482–4490.
32. **McCaughan, G. W., and A. Zekry.** 2002. Pathogenesis of hepatitis C virus recurrence in the liver allograft. Liver Transplant. **8:**s7–s13.
33. **Meertens, L., C. Bertaux, L. Cukierman, E. Cormier, and T. Dragic.** 2007. Tight junction proteins claudin-1, -6 and -9 can act as cofactors for entry of the hepatitis C virus, abstr. O-31. *In* 14th International Symposium on Hepatitis C Virus and Related Viruses.
34. **Pickles, R. J., J. A. Fahrner, J. M. Petrella, R. C. Boucher, and J. M. Bergelson.** 2000. Retargeting the coxsackievirus and adenovirus receptor to the apical surface of polarized epithelial cells reveals the glycocalyx as a barrier to adenovirus-mediated gene transfer. J. Virol. **74:**6050–6057.
35. **Pileri, P., Y. Uematsu, S. Campagnoli, G. Galli, F. Falugi, R. Petracca, A. J. Weiner, M. Houghton, D. Rosa, G. Grandi, and S. Abrigani.** 1998. Binding of hepatitis C virus to CD81. Science **282:**938–941.
36. **Reynolds, G. M., H. J. Harris, A. Jennings, K. Hu, J. Grove, P. F. Lalor, D. H. Adams, P. Balfe, S. G. Hübscher, and J. A. McKeating.** Hepatitis C virus receptor expression in normal and diseased liver tissue. Hepatology, in press.
37. **Rodriguez, J. R., D. Rodriguez, and M. Esteban.** 1991. Interferon treatment inhibits early events in vaccinia virus gene expression in infected mice. Virology **185:**929–933.
38. **Roh, M. H., C. J. Liu, S. Laurinec, and B. Margolis.** 2002. The carboxyl terminus of zona occludens-3 binds and recruits a mammalian homologue of discs lost to tight junctions. J. Biol. Chem. **277:**27501–27509.
39. **Scarselli, E., H. Ansuini, R. Cerino, R. M. Roccasecca, S. Acali, G. Filocama, C. Traboni, A. Nicosia, R. Cortese, and A. Vitelli.** 2002. The human scavenger receptor class B I is a novel candidate receptor for the hepatitis C virus. EMBO J. **21:**5017–5025.
40. **Seppen, J., S. C. Barry, J. H. Klinkspoor, L. J. Katen, S. P. Lee, J. V. Garcia, and W. R. Osborne.** 2000. Apical gene transfer into quiescent human and canine polarized intestinal epithelial cells by lentivirus vectors. J. Virol. **74:**7642–7645.
41. **Sonoda, N., M. Furuse, H. Sasaki, S. Yonemura, J. Katahira, Y. Horiguchi, and S. Tsukita.** 1999. Clostridium perfringens enterotoxin fragment removes specific claudins from tight junction strands: evidence for direct involvement of claudins in tight junction barrier. J. Cell Biol. **147:**195–204.
42. **Stevenson, B. R., and B. H. Keon.** 1998. The tight junction: morphology to molecules. Annu. Rev. Cell Dev. Biol. **14:**89–109.
43. **Tang, Y. W., S. E. Sefers, and L. Haijing.** 2005. Primer sequence modification enhances hepatitis C virus genotype coverage. J. Clin. Microbiol. **43:** 3576–3577.
44. **Timpe, J. M., Z. Stamataki, A. Jennings, K. Hu, M. J. Farquhar, H. Harris, A. Schwarz, I. Desombere, G. Leroux Roels, P. Balfe, and J. A. McKeating.** 16 October 2007. Hepatitis C virus cell-cell transmission in hepatoma cells in the presence of neutralizing antibodies. Hepatology [Epub ahead of print.] doi:10.1002/hep.21959.
45. **Wakita, T., T. Pietschmann, T. Kato, T. Date, M. Miyamoto, Z. Zhao, K. Murthy, A. Habermann, H. G. Krausslich, M. Mizokami, and R. Bartenschlager.** 2005. Production of infectious hepatitis C virus in tissue culture from a cloned viral genome. Nat. Med. **11:**791–796.
46. **Walters, R. W., P. Freimuth, T. O. Moninger, I. Ganske, J. Zabner, and M. J. Welsh.** 2002. Adenovirus fiber disrupts CAR-mediated intercellular adhesion allowing virus escape. Cell **110:**789–799.
47. **Walters, R. W., W. van't Hof, S. M. Yi, M. K. Schroth, J. Zabner, R. G. Crystal, and M. J. Welsh.** 2001. Apical localization of the coxsackie-adenovirus receptor by glycosyl-phosphatidylinositol modification is sufficient for adenovirus-mediated gene transfer through the apical surface of human airway epithelia. J. Virol. **75:**7703–7711.
48. **Wang, L., and J. L. Boyer.** 2004. The maintenance and generation of membrane polarity in hepatocytes. Hepatology **39:**892–899.
49. **Yáñez-Mó, M., R. Tejedor, P. Rousselle, and F. Sánchez-Madrid.** 2001. Tetraspanins in intercellular adhesion of polarized epithelial cells: spatial and functional relationship to integrins and cadherins. J. Cell Sci. **114:**577–578.
50. **Zheng, A., F. Yuan, Y. Li, F. Zhu, P. Hou, J. Li, X. Song, M. Ding, and H. Deng.** 2007. Claudin-6 and claudin-9 function as additional coreceptors for hepatitis C virus. J. Virol. **81:**12465–12471.
51. **Zhong, J., P. Gastaminza, G. Cheng, S. Kapadia, T. Kato, D. R. Burton, S. F. Wieland, S. L. Uprichard, T. Wakita, and F. V. Chisari.** 2005. Robust hepatitis C virus infection in vitro. Proc. Natl. Acad. Sci. USA **102:**9294–9299.